

MASGOMAS project: Two new obscured, massive and young Galactic clusters

S.A. Ramírez Alegría^{1,2}, A. Herrero^{1,2}, and A. Marín-Franch³

¹ Instituto de Astrofísica de Canarias (IAC)

² Universidad de La Laguna (ULL)

³ Centro de Estudios de Física del Cosmos de Aragón (CEFCA)

Abstract

We present two new massive clusters, discovered during the second phase of our MASGOMAS project (MAssive Stars in Galactic Obscured MAssive clusterS). The second phase of the project focuses on a systematic search of OB-type star candidates over-densities. We also present new near-infrared photometry (J , H , and K_S) and mid-resolution follow-up spectroscopy (H and K), obtained with LIRIS at ORM (La Palma), for the stellar content of the new massive clusters. With these data we have confirmed that Masgomas-1, the first candidate discovered by us, is a young and massive cluster, probably exceeding $10^4 M_\odot$, which hosts both an OB-type and an RSG populations. We have also determined the cluster distance and extinction, placing it in the Scutum-Centaurus arm, but far from the arm base (where RSGC1, RSGC2, RSGC3, Alicante 8 and Alicante 10 clusters are located), and closer to the Sun. For our second new massive cluster candidate (Masgomas-4), we have spectroscopically confirmed the presence of a massive stellar population, and photometrically detected a group of massive pre-stellar objects (Herbig Ae/Be candidates). With the estimated individual distances for the cluster massive stars, we have derived a single distance for both cores, confirming that Masgomas-4 is a single young cluster.

1 Introduction

Massive stars ($M > 8 M_\odot$) are key in the galactic evolution. During their existence, they can ionize the interstellar medium with their UV radiation, to change its chemical balance and to add it mechanical energy through their massive winds and, in their last supernova explosion, to enrich the medium with metals [13].

These massive objects are rare; for every 100 stars with a mass between 1 and $2 M_\odot$, we should expect six stars in the mass range $8 - 16 M_\odot$, and less than four with mass $M > 16 M_\odot$

[23]. Massive stars also evolve quickly, have short lifetimes and spend less time in the main sequence, compared with intermediate or low-mass stars.

In spite of their quick evolution, massive stars can be found embedded in their natal cloud even during 15% of their lifetime [3]. The extinction produced by the natal cloud and the interstellar dust makes almost impossible their detection using visual bands, therefore it is necessary to use near-infrared data, spectral range less affected by the extinction compared with optical range.

Because most of the stars are formed into clusters [16], stellar clusters are an excellent laboratory for the study of stars. In the case of massive stars, we expect to find them mostly into massive stellar clusters ($M_T > 10^4 M_\odot$). Although these objects host the most massive and luminous stars in the Galaxy, we still know just less than a dozen of them. The recent use of infrared photometric surveys such as DENIS [8], 2MASS [19], GLIMPSE [2], and UKIDSS [12], have given a boost to the discovery of obscured massive stellar clusters in the Milky Way. The exploration of highly reddened galactic regions has allowed to understand that our Galaxy is an active stellar formation machine [10], and the main cogs are the massive clusters and their massive stellar population.

Even if we have experienced a boost in the discovery of Galactic massive stellar clusters, hundreds of these objects still remain unknowns. We should expect more than 100 clusters as massive as 30 Doradus [11] and the expected number of stellar clusters would be as high as 20000 objects [10]. There is an evident difference between the expected and observed number of clusters, and this gap could be reduced thanks to projects dedicated to the systematic search and characterization of young and massive clusters around stellar formation regions.

2 Systematic search

The present phase of our MASGOMAS project [17] is dedicated to build up a systematic search of young and massive cluster candidates. In the preliminary version of the searching algorithm, we have based the OB-type star candidate selection on three photometric criteria:

1. K_S magnitude less than 12: By defining this limiting magnitude we aimed to prevent Poisson noise, derived from the field stellar distribution, from prevailing over the candidate over-densities.
2. Red ($J - K_S$) colours: Unreddened foreground disc stars exhibit bluer colours in the CMD. To eliminate most of these stars from the systematic search, we applied a cut in ($J - K_S$), discarding objects with $(J - K_S) < 0.5$.
3. Reddening-free parameter $Q_{IR} \sim 0$: The reddening-free parameter Q_{IR} [5, 14], defined as:

$$Q_{IR} = (J - H) - \frac{E(J - H)}{E(H - K_S)} \cdot (H - K_S) \quad (1)$$

has a value close to zero for OB stars. Considering photometric errors we define a range for Q_{IR} where OB-star candidates would be expected. However, because A- and

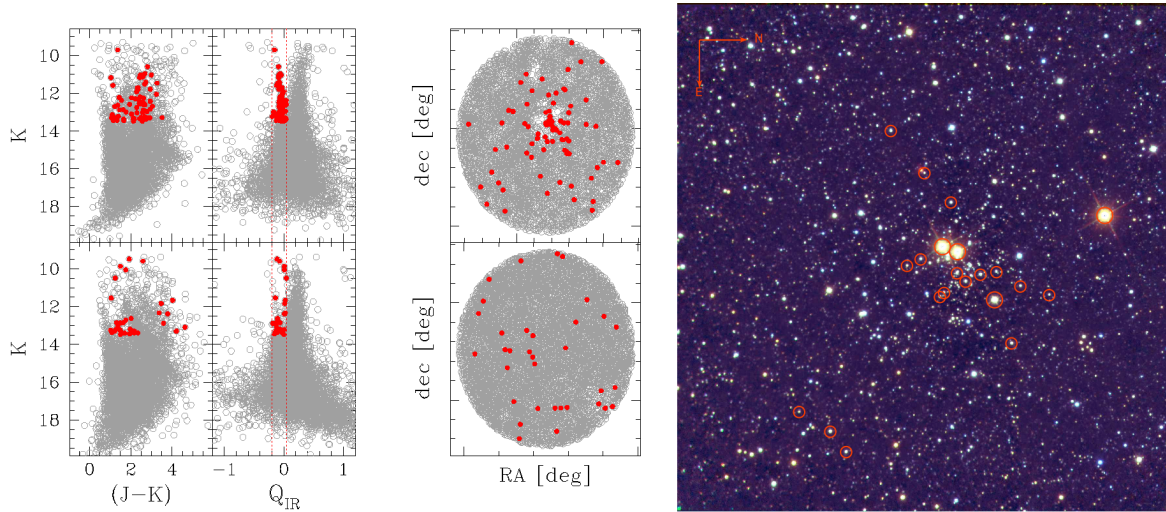


Figure 1: *Left panel:* Colour-magnitude, pseudocolour-magnitude and spatial distribution diagrams for Masgomas-1 (top) and the control field (bottom). OB-type candidates selected from our photometric cuts are presented in red dots. The concentration of OB-type candidates is evident in both the QMD (as a vertical sequence around $Q_{IR} \sim 0$) and the spatial distribution diagram of Masgomas-1. *Right panel:* Masgomas-1 false colour (LIRIS J =blue, H =green, and K_S =red) image. Spectroscopically confirmed massive stars are marked with red circles.

early F-type stars can mimic the Q_{IR} of an OB star, contamination by these stellar types is plausible. This parameter also allows to differentiate OB-type stars from low-mass/giant stars¹.

An example of the photometric cuts used for the detection of OB-candidate over-densities is shown in Fig. 1, left panel. In a quick exploration for this preliminary version we have found three previously unidentified massive clusters candidates, from which we have selected two for deep near-IR spectrophotometric follow-up: Masgomas-1, and Masgomas-4.

3 Clusters analysis

For our study we use LIRIS² near-infrared imaging (J , H , K_S), medium resolution multi-object spectroscopy (H and K) and long-slit spectroscopy (H and K).

Image data reduction (bad-pixel mask, flat correction, sky subtraction and alignment) was made with FATBOY [7] and geometrical distortions were corrected with the LIRIS reduc-

¹The value of $E(J-H)/E(H-K_S)$ varies according to the used extinction law. In our case, using Rieke's extinction law [18] this factor is 1.7.

²LIRIS is an infrared camera, with a field of view of $4.2' \times 4.2'$ and a spatial scale of $0.25''$ pixel⁻¹. It is mounted at the Cassegrain focus of the 4.2 m William Herschel Telescope, Roque de Los Muchachos Observatory, La Palma.

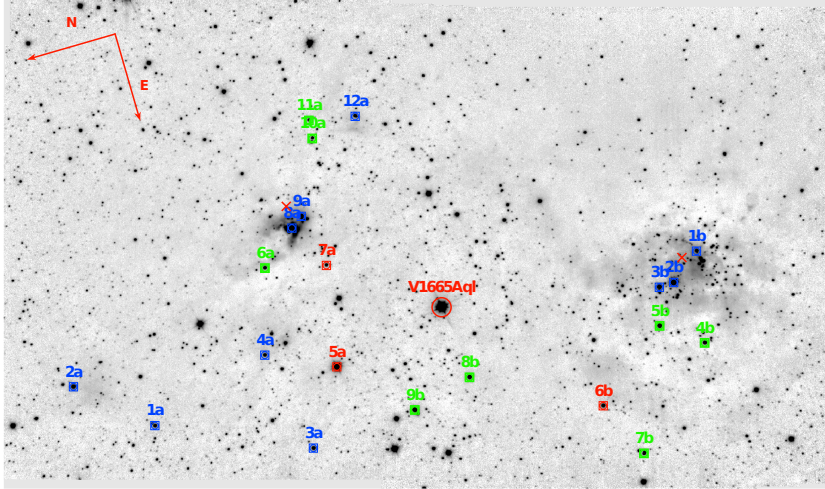


Figure 2: LIRIS K_S image for Masgomas-4. Spectroscopically observed and classified stars are marked with blue (OB-type), green (AFG dwarf stars) and red squares (giant stars). Field A and B central coordinates are marked with red crosses in the left and the right sides of the image, respectively

tion package LIRISDR. Instrumental photometry was made with DAOPHOT II, ALLSTAR and ALLFRAME [21], and was calibrated for the three filters using isolated and non-saturated stars from the 2MASS catalogue. For bright stars ($K_S < 9$ mag), we adopted the 2MASS photometry, due to saturation.

In the multi-object spectroscopic (MOS) mode, we observed mainly OB-type candidate stars, trying to keep K_S magnitude dispersion in each mask less than 2 mag; in this way we aim to obtain similar SNR for all mask stars. For bright stars, for example supergiant candidates, we prefer to use long-slit spectroscopy and pair stars with similar magnitudes. In both cases resolution were close to $\lambda/\Delta\lambda \sim 2500$.

The mask design also took into consideration the spectral range derived from the slit position. For slits located in the right half of the detector we obtain spectra from 1.55 to 1.85 μm in the H -band and from 2.06 to 2.40 μm in the K -band. These spectral ranges include the He I 1.70 μm , He I 2.11 μm , He II 2.57 μm , and He II 1.69 μm lines, which are required for early-type stellar spectral identification and classification.

Spectroscopic data reduction was done using IRAF³ for the long-slit spectra and LIRISDR, which uses the information from the mask design files, for the MOS spectra. For telluric corrections we have observed A0 V stars as telluric standards and, using XTELLCOR [22] to apply a high-resolution synthetic model of an A0 V star over the observed telluric standards, we produced the calibration spectrum with the telluric lines. This spectrum was finally used to correct our science spectra with the IRAF task TELLURIC.

³IRAF is distributed by the National Optical Astronomy Observatories, which are operated by the Association of Universities for Research in Astronomy, Inc., under cooperative agreement with the National Science Foundation.

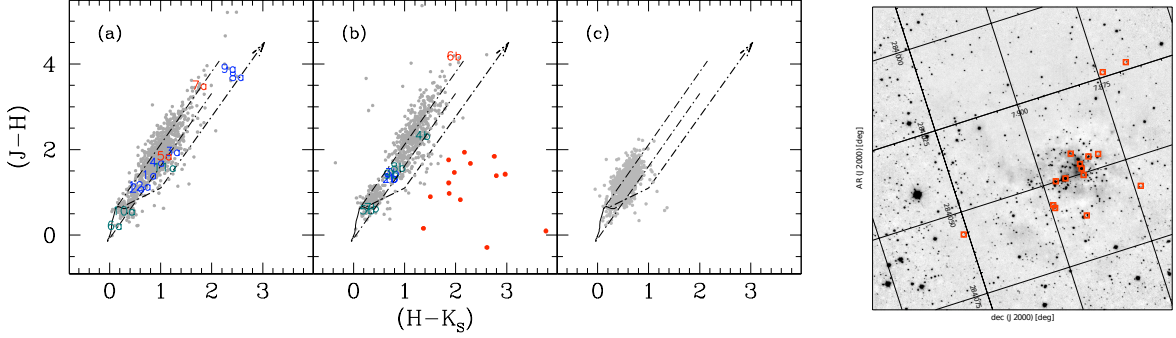


Figure 3: *Left panel:* Colour-colour diagrams for Masgomas-4 field A, B and control field. Spectroscopically observed stars are marked with numbers. Herbig Ae/Be stars from field B are marked with red dots. *Right panel:* Field B section showing the distribution of these Herbig Ae/Be candidates.

3.1 Masgomas-1

Masgomas-1 [17] (shown in Figure 1, right panel) is located in the Galactic plane, near the Scutum–Centaurus base ($l = 33.112^\circ$, $b = +0.42^\circ$, and $\alpha_{2000} = 18^{\text{h}}50^{\text{m}}15^{\text{s}}$, $\delta_{2000} = +00^\circ21'04''$). In this exciting region, where the Scutum–Centaurus arm meets the Galactic central bar, several red supergiant clusters have been found: RSGC 1 [9], RSGC 2 [6], RSGC 3 [4], and Alicante 8 [15]. These massive clusters are especially remarkable because of their population of red supergiant (RSG) stars, ranging between 8 and 26 RSGs.

For Masgomas-1 we have estimated individual distances and the associated individual extinctions for four supergiants (one yellow and three red) and 17 OB-type stars. The individual distances and extinctions are consistent with a common distance for all objects. Using the individual distance estimate, we obtained a distance to Masgomas-1 of $3.53^{+1.55}_{-1.40}$ kpc, placing Masgomas-1 in the Scutum–Centaurus arm, but far from the arm base. Therefore we can not argue in favour of a physical association between Masgomas-1 and the RSGC group.

We have also estimated the cluster total mass by adjusting a Kroupa function and integrating between 20 and $0.1 M_\odot$. Our estimate gives a cluster’s total mass of $(1.94 \pm 0.28) \cdot 10^4 M_\odot$ and this results includes Masgomas-1 in the small group of known massive clusters in the Galaxy with total mass greater than $10^4 M_\odot$.

For the cluster age we have obtained an upper limit of 10 Myr, given by the earliest dwarf star in the cluster (O9 V star), and a lower limit between 6.5 and 10 Myr, given by the presence of the M-type supergiants.

3.2 Masgomas-4

Masgomas-4 (shown in Figure 2) is located in the same direction as Masgomas-1, but at a closer distance of 1.9 kpc, as derived from the individual distance for the OB-type stars with spectroscopic observations. Field B appears particularly active in terms of massive star

formation. In the colour-colour diagrams (Fig. 3, left panel), we can see a population of stars with infrared excess, located below the region of T-Tauri objects. The position of these stars in the CCD allow us to define them as Herbig Ae/Be candidates. The presence of methanol [20] and OH masers [1] also supports an on-going massive stellar formation in the cluster.

As done for Masgomas-1, we have estimated the cluster present mass by fitting a Kroupa function and integrating in the same mass range. The result of integration gives an estimate of $(2.19 \pm 0.31) \cdot 10^3 M_{\odot}$. We have estimated the cluster age between 2 and 5 Myr, considering the presence of a surrounding H II cloud and the massive proto-stellar objects in field B.

References

- [1] Baudry, A., Desmurs, J. F., Wilson, T. L., & Cohen, R. J. 1997, *A&A*, 325, 255
- [2] Benjamin, R. A., Churchwell, E., Babler, B. L., et al. 2003, *PASP*, 115, 953
- [3] Churchwell, E. 2002, *ARA&A*, 40, 27
- [4] Clark, J. S., Negueruela, I., Davies, B., et al. 2009, *A&A*, 498, 109
- [5] Comerón, F. & Pasquali, A. 2005, *A&A*, 430, 541
- [6] Davies, B., Figer, D. F., Kudritzki, R.-P., et al. 2007, *ApJ*, 671, 781
- [7] Eikenberry, S., Elston, R., Raines, S. N., et al. 2006, *Proc. SPIE*, 6269, 626917
- [8] Epchtein, N., de Batz, B., Capoani, L., et al. 1997, *The Messenger*, 87, 27
- [9] Figer, D. F., MacKenty, J. W., Robberto, M., et al. 2006, *ApJ*, 643, 1166
- [10] Figer, D. F. 2008, in *IAU Symposium 250*, ed. F. Bresolin, P. A. Crowther, & J. Puls, 247
- [11] Hanson, M. M. & Popescu, B. 2008, in *IAU Symposium 250*, ed. F. Bresolin, P. A. Crowther, & J. Puls, 307
- [12] Lawrence, A., Warren, S. J., Almaini, O., et al. 2007, *MNRAS*, 379, 1599
- [13] Martins, F., Schaerer, D., & Hillier, D. J. 2005, *A&A*, 436, 1049
- [14] Negueruela, I. & Schurch, M. P. E. 2007, *A&A*, 461, 631
- [15] Negueruela, I., González-Fernández, C., Marco, A., Clark, J. S., & Martínez-Núñez, S. 2010, *A&A*, 513, 74
- [16] Portegies Zwart, S. F., McMillan, S. L. W., & Gieles, M. 2010, *ARA&A*, 48, 431
- [17] Ramírez Alegría, S., Marín-Franch, A., & Herrero, A. 2012, *A&A*, 541, A75
- [18] Rieke, G. H. & Lebofsky, M. J. 1985, *ApJ*, 288, 618
- [19] Skrutskie, M. F., Cutri, R. M., Stiening, R., et al. 2006, *AJ*, 131, 1163
- [20] Szymczak, M., Hrynek, G., & Kus, A. J. 2000, *A&AS*, 143, 269
- [21] Stetson, P. B. 1994, *PASP*, 106, 250
- [22] Vacca, W. D., Cushing, M. C., & Rayner, J. T. 2003, *PASP*, 115, 389
- [23] Zinnecker, H. & Yorke, H. W. 2007, *ARA&A*, 45, 481